J Am Oil Chem Soc (2014) 91:1783–1792
DOI 10.1007/s11746-014-2526-y

ORIGINAL PAPER

Structure and Physical Properties of Organogels Developed by Sitosterol and Lecithin with Sunflower Oil

Lijuan Han · Lin Li · Bing Li · Lei Zhao · Guo-qin Liu · Xinqi Liu · Xuede Wang

Received: 25 January 2014 / Revised: 16 June 2014 / Accepted: 7 August 2014 / Published online: 19 August 2014

Abstract High linoleic acid sunflower oil (*HLSO*) with various sitosterol (*Sit*) to lecithin (*Lec*) mass ratios (i.e., 0:100–100:0) were used to develop organogels at two storage temperatures (T_s: 5 and 25 °C). The results showed that, at 25 °C, the hardness value of organogels obtained from *HLSO* with both *Sit* and *Lec* was higher than that of organogels developed from *HLSO* with only *Sit* or *Lec*. Microscopy revealed that the shapes of the crystals in the organogels varied significantly with the composition of the structurant and the T_s. At both T_s used, the *Sit:Lec* (80:20) system had a lower degree of supersaturation compared with the (100:0) system. X-ray diffraction (XRD) revealed that *Sit:Lec* mass ratio of 70:30, 80:20 and 100:0 had similar short spacings, and the presence of *Lec* might be adverse to the formation of *Sit* crystal in oil. Small-angel X-ray scattering (SAXS) showed that the layer thickness of *Sit/Lec/HLSO* organogel was larger than that of *Sit/HLSO* organogel. It was found that the presence of *Lec* induced the change of self-assembly structure of *Sit* in *HLSO* and caused the changes of physical properties of organogels obtained.

Keywords Organogels · Sitosterol · Lecithin · High linoleic acid sunflower oil (HLSO)

L. Han · L. Li · B. Li · G. Liu (✉) · X. Liu
College of Light Industry and Food Sciences, South China University of Technology, Guangzhou 510640, China
e-mail: liuguoqin.scut@gmail.com; guoqin@scut.edu.cn

L. Zhao
College of Food Sciences, South China Agricultural University, Guangzhou 510642, China

X. Wang
College of Food Science and Technology, Henan University of Technology, Zhengzhou 450001, China

Introduction

In the past decade, the potential of preparing oil organogels as an alternative liquid oil structuring technique has been extensively investigated, mainly due to pressures to reduce saturated fat intake and to eliminate *trans* fats from our diets [1, 2]. In these organogels, low molecular weight organogelators (LMOGs) self-assemble from the melt and grow specifically to form a 3D network that bears no resemblance to a colloidal fat crystal network [3–5]. And in most cases, the physical properties of edible oil organogels developed from mixed self-assembled components outperform that developed from the pure components [6]. Examples of such structurant mixtures are γ-oryzanol+β-sitosterol [7–10], fatty acid+fatty alcohol [11, 12], lecithin+tristearate [13].

As far as phytosterols are concerned, they have been added to certain fat products such as margarine and vegetable oils due to their efficacy in lowering cholesterol [14, 15], and there are multiple reports in the literature of structuring vegetable oils or emulsions by sitosterol (one of the phytosterols) [7–10, 16–20]. However, dispersion of single sitosterol and oil was liquid.

Lecithin is commonly used as surfactant and crystal habit modifier [21, 22], and now it is also used in the preparation of edible oil organogels [23–26]. Tamura and Ichikawa [27] studied the effect of lecithin on organogel formation of 12-hydroxystearic acid (12-HSA) with several organic solvents.

Lecithin has been also used to structure edible oil with sorbitan tri-stearate (STS) [13], and it was found through X-ray scattering measurements and NMR relaxation tests that no solid or crystalline matter was present in samples containing only lecithin and oil. And their conclusion was that the lecithin in the system functioned as a crystal

morphology modifier. Possible co-crystallization of the lecithin with STS caused the STS crystals to assume a needle-like morphology [2]. But lecithin:STS edible oil organogels had limited use as a hardstock fat replacer because the gel collapsed at approximately 30 °C and significant softening began at 15 °C [3, 13]. A combination of lecithin and α-tocopherol could also structure edible oil by altering the packing geometry to provide supramolecular structures needed for the organogelation [28].

Our earlier work has confirmed by frequency tests that mixture of *Sit/Lec/HLSO* was able to form an organogel [29]. However, there is still insufficient understanding about other characteristics of this organogel system including its morphological structure and crystalline structure (lamella and lattice), mechanical and thermal properties under the quiescent state. In addition, as understanding the precise role of structurant on organogel formation was important in designing gels with controlled microscopic structures and physicochemical properties, and since *HLSO* was structured by *Sit* and *Lec*, the aim of this work was to further study how the *Sit/HLSO* gel structure could be affected after the addition of *Lec*. It might provide us some valuable information about a model of edible oil organogel developed from a self-assemblied molecule and a surfactant.

Materials and Methods

Materials

In the present experiments, β-sitosterol (*Sit*, 75 % purity, Aladdin Reagent Database) and lecithin (*Lec*, 98 % purity, Aladdin Reagent Database) were used in combination with refined sunflower oil high in linoleic acid (*HLSO*, main fatty acids: 27.24 % $C_{18:1}$, 55.95 % $C_{18:2}$, 6.12 % $C_{16:0}$, 5.01 % $C_{18:0}$).

Methods

Sample Preparation

Sitosterol and lecithin as structurants were added to the sunflower oil at 16 % (w/w, structurants/oil, as default) total concentration, and then this mixture was heated whilst stirred in a temperature-controlled water bath at ~90 °C for 1 h to obtain complete dissolution of the solutes. The structurants were combined in various mass ratios (*Sit:Lec* 0:100, 60:40, 70:30, 80:20 and 100:0) to form organogels with *HLSO*. After this, the samples were left to crystallize at 5 °C overnight under static conditions before storage at two temperatures (i.e., $T_s = 5$ and 25 °C) for 10 days in an incubator (temperature control range 0–60 °C with an accuracy of ±0.5 °C) prior to the optical analysis, texture, DSC, XRD and SAXS analysis to ensure that adequate time was given to anneal the crystal network giving maximum structure. In this study, a relatively high concentration of structurants (16 %) was used to ensure a high signal-to-noise ratio in the analysis.

Optical Analysis

Polarized light microscopy (PLM) was used to examine the morphology of the crystallized systems. To guarantee a uniform sample thickness, two cover slips were glued to a glass microscope slide with a distance of 2.2 cm between them. The hot sample was placed within this gap of a preheated (~95 °C) glass slide, and a glass cover slip was placed over the sample such that it rested on the glued cover slips. Samples of these solutions were stored overnight at 5 °C in a standard fridge and then stored for 10 days at different T_s (i.e., 5 and 25 °C). Photomicrographs as a function of storage temperature (T_s) was obtained of the slide, with a polarized light microscope (Axioskop 40 Pol/40 A Pol; Zeiss) equipped with a color video camera.

Texture Measurements of Sit/Lec/HLSO Gels

Force–displacement curves of the organogels were obtained with a texture analyzer (TA.XT plus; Stable Microsystems, Surrey, UK) using a flat stainless cylindrical probe (6 mm diameter). Aluminium sample holder size was Φ 55 × 35 mm. The probe penetrated the product at a constant speed of 2 mm/s to a distance of 6 mm. Hardness was defined as the maximum penetration force (*N*), and each measurement was executed six times. Data were graphed with error bars indicating the standard deviation from the mean value.

Differential Scanning Calorimetry (DSC) of Sit/Lec/HLSO Gels

The melting and crystallization thermograms of solutions of sitosterol and lecithin with *HLSO* under the quiescent state were obtained by differential scanning calorimetric (DSC) using a TA Instruments Model Q 100 (TA Instruments, New Castle, DE, USA). Samples (≈6–10 mg) were sealed in aluminum pans, and heated from 20 to 150 °C at a rate of 10 °C/min, recording the heat flow as a function of temperature. After 10 min at 150 °C, the system was cooled (10 °C/min) to 20 °C. With the equipment software (TA Instruments Universal Analysis 2000, v. 4.1D), the end temperature of melt (T_{me}) and the onset temperature of the crystallization (T_{co}) were calculated with the equipment software during the

heating and cooling stages, respectively. At least two replications were done on each sample.

As reported by Lam et al. [30] and Li et al. [31], supercooling (τ, also termed supersaturated state) under isothermal conditions has been defined as:

$$\tau = (T^* - T)/T^* \quad (1)$$

where T^* is the equilibrium temperature and T is the temperature of gelation. Since the samples were gelled at 5 and 25 °C (i.e., T_s) that $T = T_s$ here, and the end melting temperature (T_{me}) was the equilibrium temperature (i.e., $T_{me} = T^*$), therefore, Eq (1) could be written as:

$$\tau = (T_{me} - T_s)/T_{me} \quad (2)$$

X-Ray Diffraction (XRD) of Sit/Lec/HLSO Gels

A Phillips diffractometer (D8 ADVANCE; Bruker AXS, German) with Cu–K_α radiation ($\lambda = 1.54056$ Å, at 40 kV and 40 mA) was used to determine the polymorphic form of the crystal network in organogels. Scans were performed at 0.02° step size at 2θ from 3° to 30° and 19.1-s acquisition time.

The short-spacing (i.e., d-space), which is the distance between diffracting planes, was calculated by substituting the scattering angle, 2θ, of the peak into the Bragg equation:

$$d = \lambda/(2\sin\theta) \quad (3)$$

where λ is the wavelength of the Cu–K_α ray and 2θ is the diffraction angle.

The relative crystallinity (X_c) was calculated by Jade 6.0 software:

$$X_c = A_c/(A_c + A_a) \quad (4)$$

where A_c is the area of the crystalline region and A_a is the area of the amorphous region.

Small Angle X-ray Scattering (SAXS) Measurements

Small-angle scattering (SAXS) experiments were performed in reflection mode on samples containing *HLSO* and structurants at different *Sit*/*Lec* mass ratios. SAXS experiments were performed using a SAXSess camera (Anton-Paar, Graz, Austria). A PW3830 X-ray generator with a long fine focus sealed glass X-ray tube (PANalytical) was operated at 40 kV and 50 mA. A focusing multilayer optics and a block collimator provided an intense monochromatic primary beam (Cu–Kα, wavelength 1.542 Å). A q-range is from 0.06 to 0.40 $Å^{-1}$, corresponding to 100–15.70 Å in real space. The samples were held in an aluminium sample holder (a depth of 2.2 mm) with thin mica windows. Temperature (5 and 25 °C) was controlled by Peltier elements. Data were acquired using a chip charge-coupled device camera detector. The incident and transmitted X-ray beam intensities were recorded with each SAXS pattern, and used to normalize the measured SAXS intensities. The corresponding background intensity was subtracted, and the resulting corrected scattered intensity was denoted by $I(q)$.

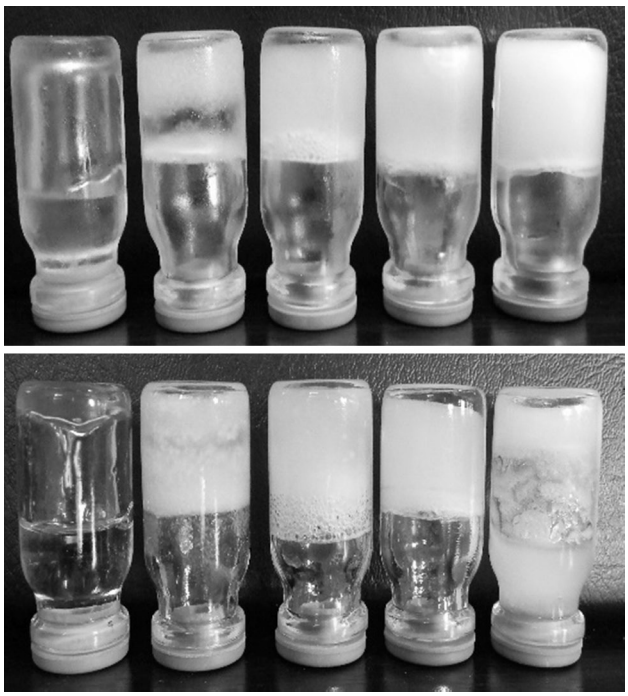

Fig. 1 Mixtures of sitosterol+lecithin in *HLSO* in various mass ratios (from *left* to *right*: *Sit*:*Lec* 0:100, 60:40, 70:30, 80:20, 100:0) at two T_s: 5 °C (*top*) and 25 °C (*bottom*)

Results and Discussion

Microstructure and Texture Measurements of Organogels After Storage.

Figure 1 captured the appearance of the mixtures of sitosterol+lecithin in *HLSO* in various mass ratios at two T_s after 10 days of storage. When mass ratio of *Sit*-to-*Lec* was between 0:100 and 60:40, there might be some sedimentation of crystals or phase separation in these supersaturated solutions (except *Sit:Lec* 100:0 at 5 °C), but not at a sufficient level to create a space filling network that resulted into a gel-like structure. So these systems should not be further analyzed, however, for comparison between different organogels, individual structurants with *HLSO* (i.e., *Sit:Lec* 0:100 and 100:0 organogels) would not be excluded from analysis. It was noted that the transparency of the pure *Sit* with *HLSO* was lower than that of *Sit/Lec/HLSO* samples and pure *Lec* with *HLSO*, which confirmed that the cloudiness of the samples was due to *Sit*.

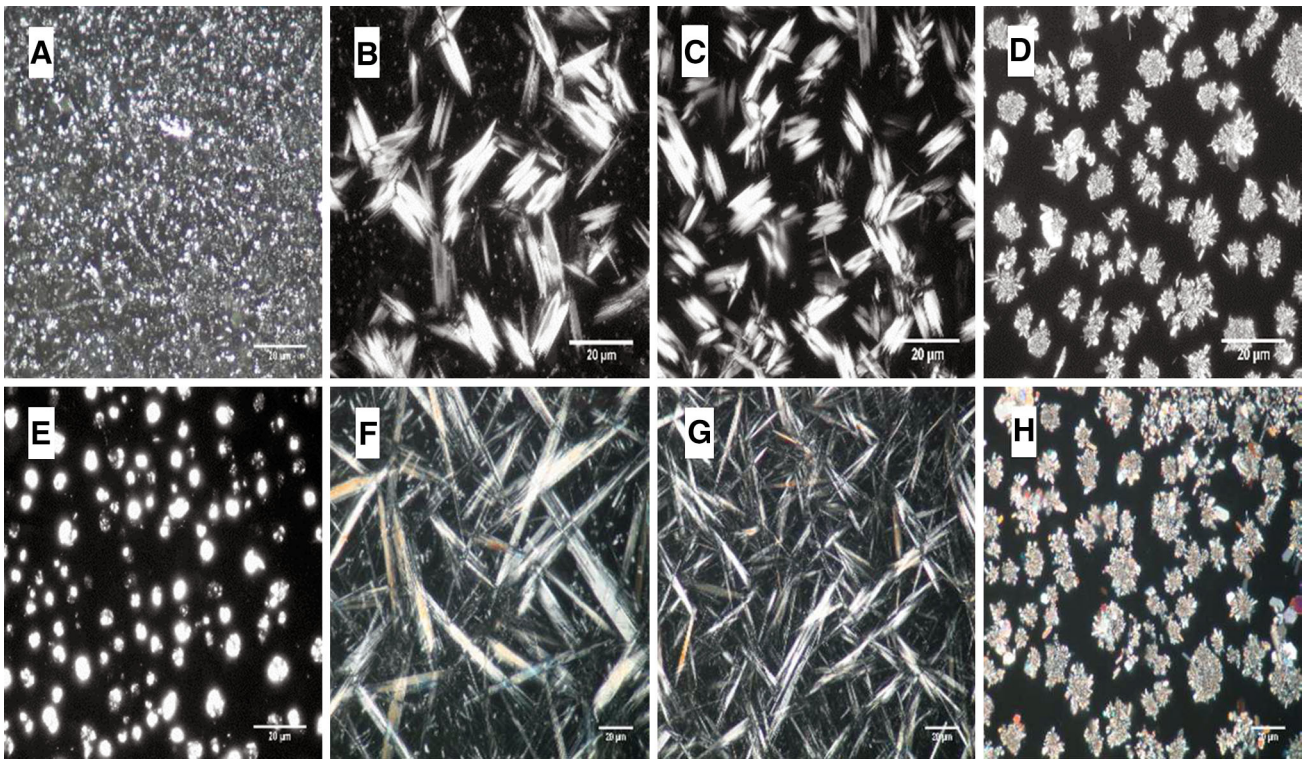

Fig. 2 PLM images of crystalline network of **a–d** denoted *Sit*:*Lec* 0:100, 70:30, 80:20, 100:0 organogels at 5 °C; and **e–h** denoted *Sit*:*Lec* 0:100, 70:30, 80:20, 100:0 organogels at 25 °C. *Scale bar* 20 μm

Examination of *Sit/Lec/HLSO* organogels under a PLM was shown in Fig. 2. At 5 or 25 °C, there were crystals in pure *Lec* with *HLSO*. Since the morphology of crystal network in other samples had been described in our previous study [29], it would be a brief description here. Pure *Sit* with *HLSO* had a uniform crystal structure, which contained a single supramolecular morphology (rosette-shaped). But a drastic to feather or needle-like change in the crystal morphology occurred when *Lec* was added. In the *Sit*/*Lec*/*HLSO* systems, the presence of *Lec* might cause changes in the self-assembly route (or direction) of *Sit* in *HLSO*.

After the samples became solid-like, texture measurement was applied to determine the firmness of organogels. Figure 3 showed the effect of mass ratio between *Sit* and *Lec* on the hardness of organogels developed at two storage temperatures. At a comparable structurant composition, the hardness of the organogel developed at lower storage temperature was higher than the hardness of the one at higher temperature, e.g., the hardness for *Sit:Lec* (80:20) organogel stored at 5 °C was twice as high as for the 25 °C counterparts. It can be seen from the PLM images that the microcrystalline particles formed at 5 °C were smaller and had thicker strands and larger pores than the microstructures formed at T_s of 25 °C (Fig. 2). As it has been documented that the smaller size of the primary particles that

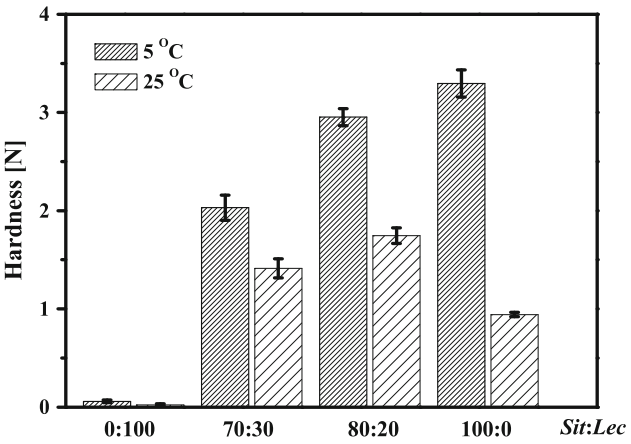

Fig. 3 Effect of structurant composition on the hardness of organogels at two T_s (5 and 25 °C). *Error bars* standard deviations from the mean

formed a three-dimensional network, the higher firmness of the system [32–35], and gels with thicker strands and larger pores were able to withstand greater amounts of mechanical stress [36], thus harder samples were obtained at 5 °C. Also, a higher firmness usually results from higher degree of crystallinity (X_c) in the system that triacylglycerides play an important role, i.e., chocolate, butter, margarine [35, 37].

At T_s of 5 °C, the hardness values of organogels increased continuously with increasing the *Sit* content in the system, while at 25 °C, a clear difference between the organogels developed from *HLSO* with pure components and the mixed structurants was noticeable (i.e., there was a synergetic effect between two structurants on hardness of organogels at higher storage temperature). For example, the hardness of organogel increased from about 0.94 to 1.75 *N* as the structurants composition changed from *Sit:Lec* mass ratio of 100:0 to 80:20. The variation of the organogels' hardness at high storage temperature could not be just associated with crystallinity like that at low storage temperature. The structural characteristics of the organogels (i.e., average size and shape of the solid particles, the solid–liquid surface energy, the particle–particle interactions, and the three-dimensional organization of the solid phase) had to be taken into account in explaining the increase in the organogels' hardness [32–35]. The microphotographs obtained by PLM (Fig. 2) showed that at T_s of 25 °C, organogels obtained from the mixture of *Sit* and *Lec* with oil had a needle-like structure (which always results in better structuring ability) and showed higher level of three-dimensional crystal organization than the organogels developed by *Sit/HLSO* (Fig. 2), which corresponded to a higher interaction between crystalline particles. It can be speculated that the hardness of organogels formed at high storage temperature in this work was more related to the microstructural characteristics than the amount of crystals (i.e., X_c), providing indirect evidence that the presence of *Lec* in the system altered the 3D network microstructure formed by *Sit/HLSO* and, therefore, the organogels textures. So, based on the discussion above, the hardness of *Sit/Lec/HLSO* organogels depended on both storage temperature and structurant composition.

Thermal Behaviors of Organogels

The information of melting behavior for different organogels under the dynamic deformation state (i.e., the melting point determination of organogels after a period of storage using a rheological method) had been assessed in our previous study [29]. And in this study, the melting thermograms and crystallization thermograms for some *Sit/Lec/HLSO* solutions and organogels under the quiescent state were recorded (Fig. 4). The melting curves did not show any pronounced endothermic peak, especially at the higher storage temperature (Fig. 4c), indicating that there was less crystalline mass presented at the elevated temperature. It must be pointed out that, although no distinct evidence of crystal melting behavior was found in any of the tested organogel samples, structurants were undoubtedly crystalline on the evidence of optical microscopy and outward appearances.

No exothermic peaks could be recognized in the cooling curves of *Sit:Lec* (0:100) and (70:30) organogels. This might be caused by too much *Lec* which would greatly increase the solubility of *Sit* in *HLSO*, and might result in a too slow nucleation rate which could not be detected by the DSC method, so that there was no obvious crystallization exothermic peak in *Sit:Lec* (70:30) organogels. In the other two organogels (i.e., *Sit:Lec* 80:20 and 100:0 organogels), as the content of *Lec* decreased or the storage temperature increased, an increase of the onset of crystallized temperature (T_{co}) of the corresponding organogels was observed. The T_{co} of *Sit:Lec* (80:20) organogel at T_s of 5 and 25 °C was 59 and 75 °C, and the T_{co} of *Sit:Lec* (100:0) organogel at 5 and 25 °C was 72 and 80 °C, respectively. Different structurants composition of organogel corresponded to different degrees of supersaturation, and the end melting temperature for *Sit:Lec* (80:20) and *Sit:Lec* (100:0) in *HLSO* were about 85 and 100 °C, respectively. Therefore, according to Eq. 2, the supercooling τ for organogel stored at 5 °C, $\tau_{80:20} = 0.94$, $\tau_{100:0} = 0.95$; and for 25 °C, $\tau_{80:20} = 0.71$, $\tau_{100:0} = 0.75$. It could be seen that, at each T_s, *Sit:Lec* (80:20) organogel had a low degree of supersaturation compared with *Sit:Lec* (100:0) organogel, and the crystallographic mismatch nucleation barrier was higher than *Sit:Lec* (100:0) organogel, favoring one-dimensional growth of crystals [30]. This observation was in accordance with the PLM results that the crystals in the *Sit:Lec* (80:20) system grew one-dimensionally with rare branching. Moreover, for the *Sit:Lec* (80:20) organogel, the degree of supersaturation decreased with increasing storage temperature, thus the crystalline unit in *Sit:Lec* (80:20) organogel at 25 °C was longer than at 5 °C (Fig. 2c, g) [30].

X-ray Diffraction and Small-Angle X-ray Scattering

To determine whether differences in the visual appearance and macroscopic properties of the organogels described in the front at different storage temperatures and structurant compositions were due to the presence of different polymorphs of structurants, powder X-ray diffraction (Fig. 5) and small-angle X-ray scattering (Fig. 6) were employed. All the results were without deduction of the contribution due to the *HLSO*. And it should be noted that the *Sit:Lec* (0:100) solutions/dispersions did not form gels, so the diffractograms and scattering patterns of this series of solutions/dispersions should not be expected to be completely quantitative in terms of peak intensities [8].

XRD were used to evaluate the molecular assembly of the structurants forming those crystals, as part of the explanation of the observed phenomena. In the current work, the X-rays were diffracted through a diluted system,

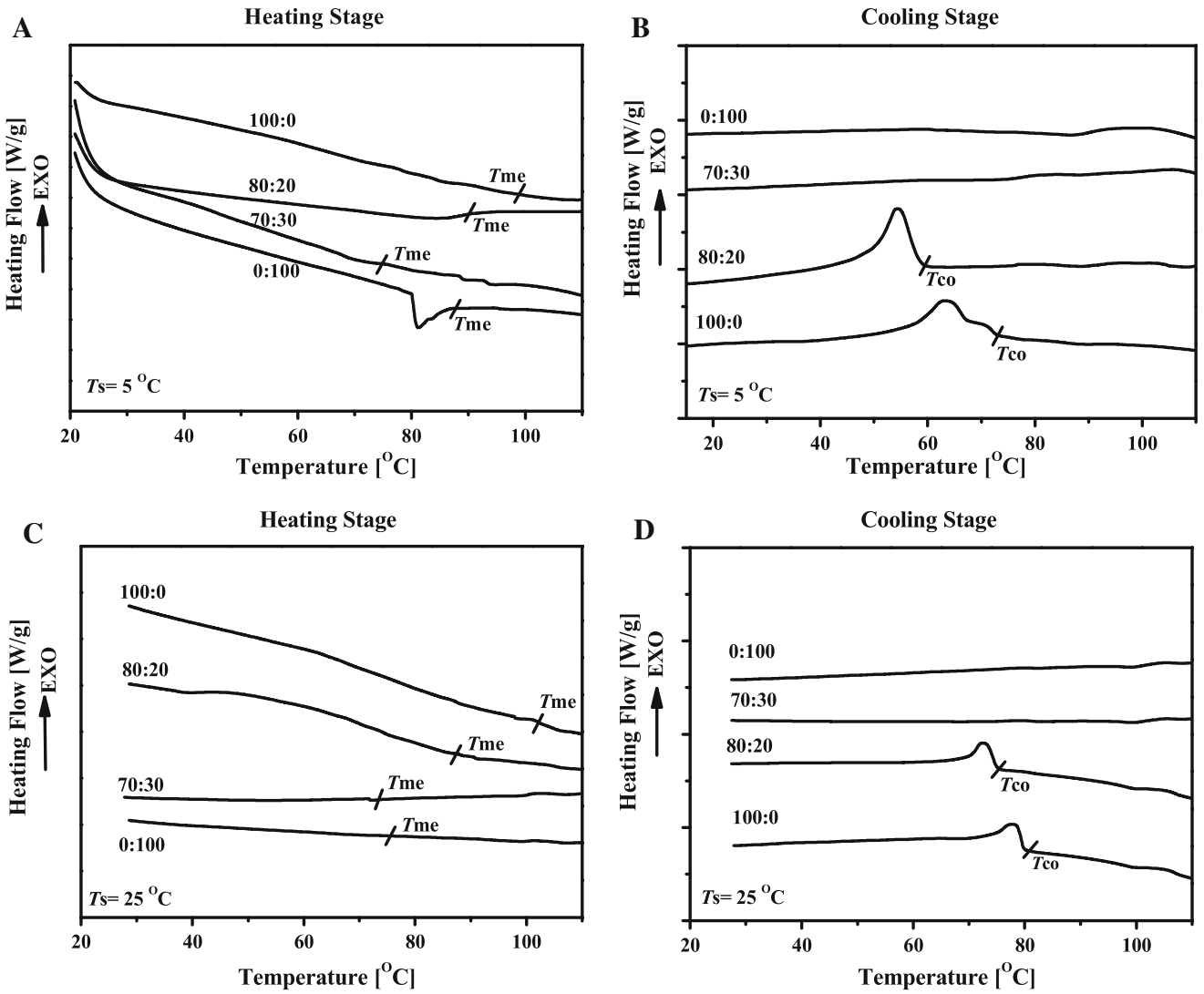

Fig. 4 Effect of *Sit*:*Lec* mass ratio on the T_{me} and T_{co} of organogels as obtained by DSC at a heating/cooling rate 10 °C/min. Curves were shifted for clarity. *Left panel* shows the heating stage: **a** $T_s = 5$ °C and **c** $T_s = 25$ °C. *Right panel* shows the cooling stage with curves in inverted order: **b** $T_s = 5$ °C and **d** $T_s = 25$ °C

in which the solids were considered a powder. The XRD patterns for only *Lec* with *HLSO* or *Sit* with *HLSO* (i.e., *Sit:Lec* mass ratio of 0:100 and 100:0), and organogels stored at different temperatures with various structurant compositions are shown in Fig. 5. The peaks identified in Fig. 5 corresponded to those spacings for the organogels were summarized in Table 1.

At large reflection angles (2θ), one wide diffraction peak centered at 2θ of 20° (corresponding to *d* spacing of 4.44 Å) was observed for *Lec* with *HLSO*, (Fig. 5, *Sit:Lec* 0:100). This wide diffraction peak might be caused by the diffraction of oil [38], and it could be observed in all the organogels analyzed since the diffraction background caused by oil had not been subtracted. *Lec* with *HLSO* also gave two clear peaks at small angel of $2\theta = 5.48°$ and 7.34°, corresponding to *d* values of 16.108 and 12.025 Å, respectively.

Sit with *HLSO* gave a very strong peak at small angle of $2\theta = 4.71°$ at 5 °C and 4.76° at 25 °C, corresponding to *d* value of 18.75 and 18.55 Å, respectively, and followed by at least ten minor peaks within the scanned range. This major diffraction peak was also present in the mixed structurants with *HLSO* but with different diffraction intensity (Fig. 5, *Sit:Lec* 70:30 and 80:20 organogels), and no significant changes in peak position were observed at 5 °C, while a shift towards slightly larger *d* spacing at 25 °C was observed.

It was observed that the X-ray spectra for the *Sit* with *HLSO* and the mixed structurants with *HLSO* (i.e., *Sit:Lec* 70:30 and 80:20 organogels) were similar, all showing

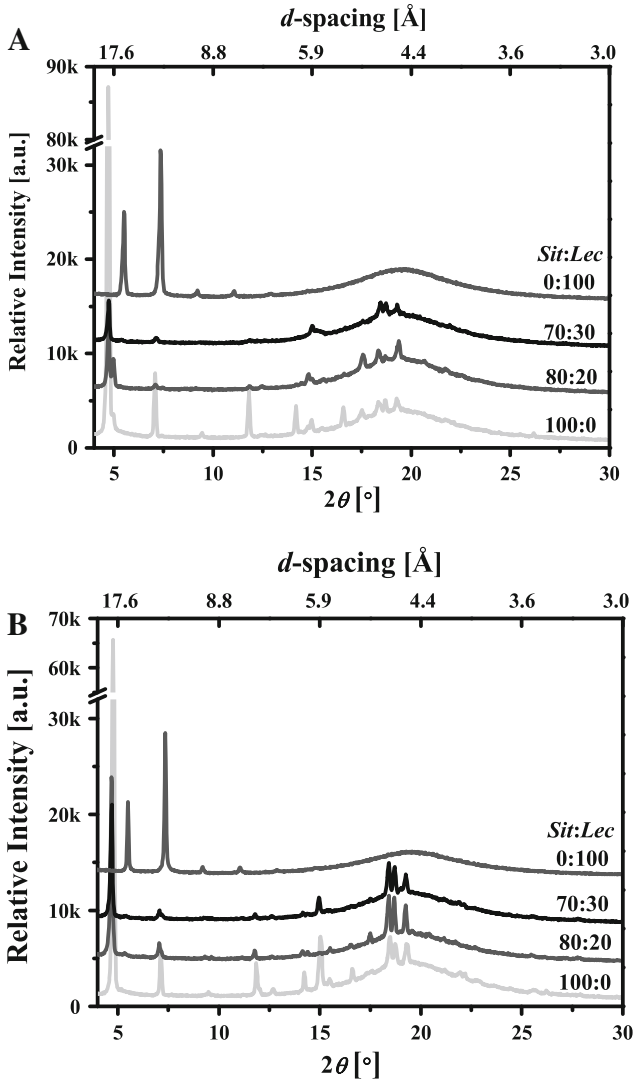

Fig. 5 X-ray diffraction profiles for organogels at $T_s = 5$ °C (**a**) and $T_s = 25$ °C (**b**) as a function of the structurant composition. The diffraction profiles were shifted vertically for clarity. All measurements were done at room temperature

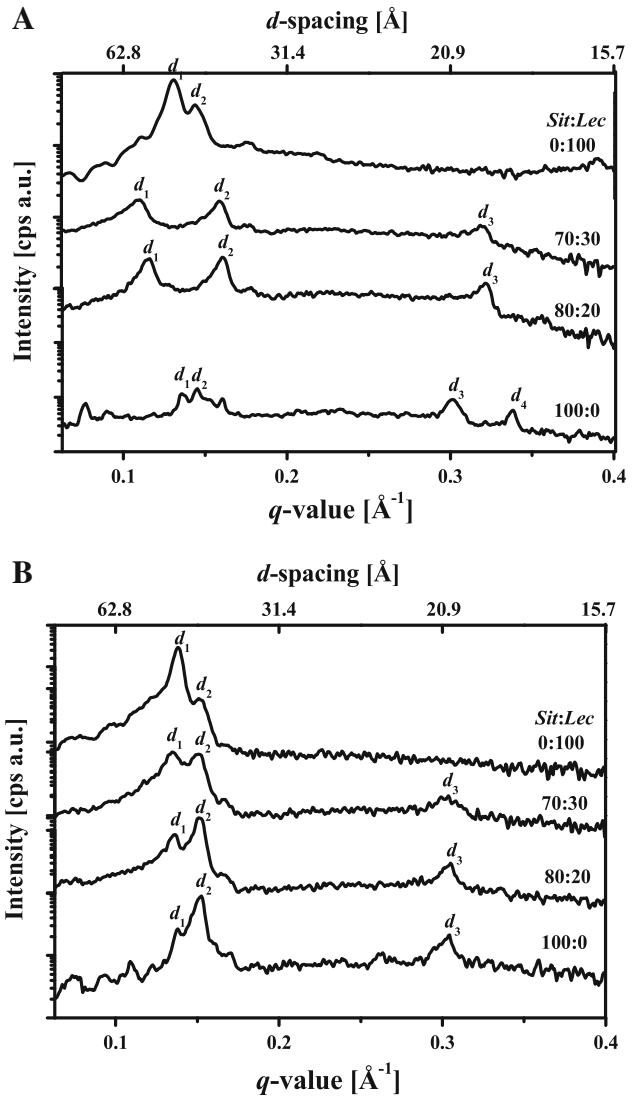

Fig. 6 Log $I-q$ SAXS patterns of oil+*Sit*/*Lec* system at $T_s = 5$ °C (**a**) and $T_s = 25$ °C (**b**) as a function of the structurant composition

short spacings around 4.82, 4.75 and 4.58 Å, suggesting a relationship between the molecular packing in the *Sit*/*HLSO* and *Sit*/*Lec*/*HLSO* organogels, i.e., the addition of *Lec* did not alter the diffraction spectra observed in the *Sit*:*Lec* 100:0 organogels. This also indicated that the presence of *Lec* at the temperature conditions investigated (5 and 25 °C) did not change the *d* spacing or the subcell packing of the *Sit* crystals in the organogels. However, a series of peaks at 2θ between 6° and 15° in *Sit*:*Lec* 100:0 organogel was absent in the *Lec* co-existed organogels (Fig. 5), indicating some ordered structures with the corresponding short spacings to these peaks disappeared after the addition of *Lec*.

As the *Sit*-rich organogels had higher degree of supersaturation at both T_s (according to the DSC data), a larger *Sit* content yielded a larger number of crystals, so it was reasonable that the crystallinity increased with increasing *Sit* content in the structurants mixture (as presented in Fig. 5; Table 1), which suggested the presence of *Lec* was adverse to the formation of *Sit* crystal. It might be thought that when an increasing ratio of *Lec* was present in the structurants mixture, the relative ratio of *Sit* would decrease accordingly. As a result, the amount of formed *Sit* crystal declined. However, the increase in *Sit* content in the system was disproportionate to the increase in the crystallinity in the system, i.e., the actual crystallinity value of the *Sit*:*Lec* (80:20) organogel corresponding to the crystallization of *Sit* in *HLSO* was much less than its theoretical value [calculated from the crystallinity value of the *Sit*:*Lec* (100:0) organogel, whose crystallinity was totally contributed by *Sit* crystals], which suggested the presence of *Lec* was adverse to the formation

Table 1 X-ray diffraction of *Sit*/*Lec-HLSO* organogels with different structurant composition at 5 and 25 °C

Samples	X_c (%)	$2\theta_{\text{first peak}}$ (°)	*d*-spacing (Å)
Sit:*Lec* (0:100), 5 °C	22.80 ± 1.63	5.48	16.11
Sit:*Lec* (70:30), 5 °C	13.25 ± 1.32	4.72	18.71
Sit:*Lec* (80:20), 5 °C	20.85 ± 1.63	4.71	18.75
Sit:*Lec* (100:0), 5 °C	46.90 ± 5.49	4.71	18.75
Sit:*Lec* (0:100), 25 °C	22.50 ± 2.79	5.48	16.11
Sit:*Lec* (70:30), 25 °C	22.80 ± 7.77	4.68	18.87
Sit:*Lec* (80:20), 25 °C	28.25 ± 2.37	4.68	18.87
Sit:*Lec* (100:0), 25 °C	44.95 ± 10.54	4.76	18.55

X_c relative crystallinity

Table 2 SAXS of *Sit*/*Lec-HLSO* organogels obtained at different storage temperature and structurant composition

Samples	d_1 (Å)[a]	d_2 (Å)[a]	d_3 (Å)[a]	d_4 (Å)[a]
Sit:*Lec* (0:100), 5 °C	48.03 *s*[b]	43.62 *w*[b]	–	–
Sit:*Lec* (70:30), 5 °C	56.61 *m*[b]	39.46 *m*	19.69	–
Sit:*Lec* (80:20), 5 °C	54.34 *m*	39.30 *m*	19.57	–
Sit:*Lec* (100:0), 5 °C	46.39 *w*	43.23 *w*	20.83	18.58
Sit:*Lec* (0:100), 25 °C	45.50 *s*	41.53 *w*	–	–
Sit:*Lec* (70:30), 25 °C	46.62 *m*	41.71 *m*	20.68	–
Sit:*Lec* (80:20), 25 °C	46.16 *m*	41.53 *m*	20.59	–
Sit:*Lec* (100:0), 25 °C	45.50 *w*	41.17 *s*	20.63	–

s strong, *m* medium, *w* weak

[a] $d = 2\pi/q$

[b] Scattering intensity

of *Sit* crystal in *HLSO*. And it was intersting to note that the mixed structurants with *HLSO* developed organogels (i.e., the *Sit:Lec* 70:30 and 80:20 organogels) at lower X_c (indicating the solid phase content in the system) than only *Sit* with oil at 5 °C, which might suggest that *Sit* had higher solubility with *Lec* in *HLSO* than without *Lec*, i.e., *Sit* had higher self-assembly capacity in the presence of *Lec* in *HLSO*, like that observed in candelilla wax and dotriacontane organogels [39]. Table 1 also shows that, for a given structurant composition, the amount of crystal material (i.e., X_c) at 5 °C was lower than at 25 °C (except *Sit:Lec* 100:0 gel). And this agreed with previous DSC analysis that the structurant molecules growth was easier and much more at higher storage temperature, and finally led to a higher X_c.

Scattering patterns of dispersions/organogels In order to better understand the nature of the solids observed under the microscope, X-ray scattering was performed, as shown in Fig. 6. In Fig. 6, the scattering patterns for both pure components with oil (i.e., the *Sit:Lec* 0:100 solution and *Sit:Lec* 100:0 organogel), as well as two mixed structurants with *HLSO* (i.e., the *Sit:Lec* 70:30 and 80:20 organogels) were presented, and all the corresponding to *d* values were calculated according to Bragg law and summarized in Table 2.

From Fig. 6 and Table 2, it can be seen that the *Lec*/*HLSO* (i.e., the *Sit:Lec* 0:100 solution) showed the first order reflection d_1 48.03 Å at 5 °C and 45.50 Å at 25 °C, followed by a weaker shoulder at higher *q* value (d_2 43.62 Å at 5 °C and 41.53 Å at 25 °C), and the higher reflections were often hardly discernible. Therefore, based on the SAXS, X-ray diffraction tests and PLM images (Fig. 2a, e), it could be deduced that there were crystals in samples containing only *Lec* with oil, although not reaching a level to form gel. However, this was not in agreement with Pernetti et al. [13] that the lecithin solids as seen under PLM were not crystals. They put forward this conclusion because, according to their X-ray scattering measurements and NMR relaxation tests, there was no solid or crystalline matter presented in samples containing only lecithin with edible oil.

At T_s of 5 °C, the scattering spectrum of the *Sit*/*HLSO* sample [Fig. 6; Table 2, the *Sit*:*Lec* (100:0) organogel] showed a series of scattering peaks with low intensity. The presence of clear higher order reflections (d_4 18.58 Å) indicated a relatively thick crystal in the direction of the chains [11]. The first scattering peak corresponded to a layer thickness of 46.39 Å (d_1), while this peak shifted to 45.50 Å (d_1) with increasing T_s.

The layer thickness (i.e., d_1 in Table 2) of the *Sit*:*Lec* (70:30) and (80:20) organogels was more or less larger than the *Sit*:*Lec* (100:0) organogel at both T_s, indicating that the presence of *Lec* might result in this difference in the layer thickness values between different organogels. And this difference was larger between the organogels stored at low temperature than those stored at high temperature. It could also be speculated that *Lec* might make the self-assembly structure of *Sit* in the *HLSO* become loose. At 25 °C, the positions of higher order reflections (corresponding to higher *d* values; i.e., $d_2 - d_4$ in Table 2) for all the organogels were very close. While at 5 °C, d_2 and d_3 values of the *Sit*:*Lec* (70:30) and (80:20) organogels were lower than their counterparts of the *Sit*:*Lec* (100:0) organogel.

Conclusions

In the present paper, the influence of the presence of lecithin on the structure of sitosterol/*HLSO* was discussed in detail. Obtained results showed that compared with the *Sit*/*HLSO* system, an increase of the crystallographic mismatch nucleation barrier was observed on the *Sit/Lec/HLSO* system, resulting in one-dimensional growth of crystals and a more effective oil structured network, i.e., sitosterol had a

better oil structuring capacity with the help of lecithin. And, finally, these changes in the crystal morphology and network structure caused the changes of physical properties of organogels obtained, which providing us a model of modulating physical properties of edible oil organogels formed through the self-assembly of low molecular weight structurant or organogelator (e.g., *Sit*, etc.) by the addition of a surfactant (e.g., *Lec*, etc.).

Acknowledgments We would like to gratefully thank the financial support from the National Natural Science Foundation of China (Project No. 31130042; No. 31271885 and No. 31271884), Key Projects in the National Science & Technology Pillar Program during the Twelfth Five-year Plan Period (Project No. 2012BAD37B01), National Hi-tech Research and Development Project (863-SS2013AA102103) and Public Welfare (Agriculture) Research Project (201303072).

References

1. Dassanayake LSK, Kodali DR, Ueno S (2011) Formation of oleogels based on edible lipid materials. Curr Opin Colloid In 16:432–439
2. Co ED, Marangoni AG (2012) Organogels: an alternative edible oil-structuring method. J Am Oil Chem Soc 89:749–780
3. Marangoni AG, Garti N (2011) An overview of the past, present, and future of organogels. In: Marangoni AG, Garti N (eds) Edible oleogels: structure and health implications. AOCS Press, Urbana, p 9
4. Wright AJ, Marangoni AG (2006) Formation, structure, and rheological properties of ricinelaidic acid-vegetable oil organogels. J Am Oil Chem Soc 83:497–503
5. Wright AJ, Marangoni AG (2007) Time, temperature, and concentration dependence of ricinelaidic acid-canola oil organogelation. J Am Oil Chem Soc 84:3–9
6. Pernetti M, van Malssen KF, Flöter E, Bot A (2007) Structuring of edible oils by alternatives to crystalline fat. Curr Opin Colloid In 12:221–231
7. Bot A, Agterof WGM (2006) Structuring of edible oils by mixtures of γ-oryzanol with β-sitosterol or related phytosterols. J Am Oil Chem Soc 83:513–521
8. Bot A, den Adel R, Roijers EC (2008) Fibrils of γ-oryzanol+β-sitosterol in edible oil organogels. J Am Oil Chem Soc 85:1127–1134
9. Bot A, den Adel R, Roijers EC, Regkos C (2009) Effect of sterol type on structure of tubules in sterol+γ-oryzanol-based organogels. Food Biophys 4:266–272
10. Bot A, den Adel R, Regkos C, Sawalha H, Venema P, Flöter E (2011) Structuring in β-sitosterol+γ-oryzanol–based emulsion gels during various stages of a temperature cycle. Food Hydrocoll 25:639–646
11. Schaink HM, van Malssen KF, Morgado-Alves S, Kalnin D, van der Linden E (2007) Crystal network for edible oil organogels: possibilities and limitations of the fatty acid and fatty alcohol systems. Food Res Int 40:1185–1193
12. Gandolfo FG, Bot A, Flöter E (2004) Structuring of edible oils by long-chain FA, fatty alcohols, and their mixtures. J Am Oil Chem Soc 81:1–6
13. Pernetti M, van Malssen K, Kalnin D, Flöter E (2007) Structuring edible oil with lecithin and sorbitan tri-stearate. Food Hydrocolloids 21:855–861
14. Mellema M (2009) Co-crystals of beeswax and various vegetable waxes with sterols studied by X-ray diffraction and differential scanning calorimetry. J Am Oil Chem Soc 86:499–505
15. Law MR (2000) Plant sterol and stanol margarines and health. West J Med 173:43–47
16. Bot A, Veldhuizen YSJ, den Adel R, Roijers EC (2009) Non-TAG structuring of edible oils and emulsions. Food Hydrocoll 23:1184–1189
17. Christiansen LI, Rantanen JT, von Bonsdorff AK, Karjalainen MA, Yliruusi JK (2002) A novel method of producing a microcrystalline β-sitosterol suspension in oil. Eur J Pharm Sci 15:261–269
18. Rogers MA, Bot A, Lam RSH, Pedersen T, May T (2010) Multicomponent hollow tubules formed using phytosterol and γ-oryzanol based compounds: an understanding of their molecular embrace. J Phys Chem A 114:8278–8285
19. Sawalha H, Venema P, Bot A, Flöter E, van der Linden E (2011) The influence of concentration and temperature on the formation of γ-oryzanol+β-sitosterol tubules in edible oil organaogels. Food Biophys 6:20–25
20. Sawalha H, den Adel R, Venema P, Bot A, Flöter E, van der Linden E (2012) Organogel-emulsions with mixtures of β-sitosterol+γ-oryzanol: effects of water activity and type of continuous oil phase. J Agr Food Chem 60:3462–3470
21. Garti N, Schlichter J, Sarig S (1986) Effect of food emulsifiers on the polymorphic transitions of cocoa butter. J Am Oil Chem Soc 63:230–236
22. Vanhoutte B, Fourniat J, Duplacie F, Huyghebaert A, Dewettinck K (2002) Effect of phospholipids on isothermal crystallization and fractionation of milk fat. Eur J Lipid Sci Tech 104:738–744
23. Angelico R, Ceglie A, Colafemmina G, Delfine F, Olsson U, Palazzo G (2004) Phase behavior of the lecithin/water/isooctane and lecithin/water/decane systems. Langmuir 20:619–631
24. Angelico R, Ceglie A, Colafemmina G, Lopez F, Murgia S, Olsson U, Palazzo G (2005) Biocompatible lecithin organogels: structure and phase equilibria. Langmuir 21:140–148
25. Mezzasalma SA, Koper GJM, Shchipunov YA (2000) Lecithin organogel as a binary blend of monodisperse polymer-like micelles. Langmuir 16:10564–10565
26. Shchipunov YA, Mezzasalma SA, Koper GJM, Hoffmann H (2001) Lecithin organogel with new rheological and scaling behaviour. J Phys Chem B 105:10484–10488
27. Tamura T, Ichikawa M (1997) Effect of lecithin on organogel formation of 12-hydroxystearic acid. J Am Oil Chem Soc 74:491–495
28. Nikiforidis CV, Scholten E (2014) Self-assemblies of lecithin and α-tocopherol as gelators of lipid material. RSC Adv 4:2466–2473
29. Han LJ, Li L, Zhao L, Li B, Liu GQ, Liu XQ, Wang XD (2013) Rheological properties of organogels developed by sitosterol and lecithin. Food Res Int 53:42–48
30. Lam R, Quaroni L, Pederson T, Rogers MA (2010) A molecular insight into the nature of crystallographic mismatches in self-assembled fibrillar networks under non-isothermal crystallization conditions. Soft Matter 6:404–408
31. Li JL, Wang RY, Liu XY, Pan HH (2009) Nanoengineering of a biocompatible organogel by thermal processing. J Phys Chem B 113:5011–5015
32. Marangoni AG (2000) Elasticity of high-volume fraction fractal aggregate networks: a thermodynamic approach. Phys Rev Lett B 62:13951–13955
33. Marangoni AG, Rogers MA (2003) Structural basis for the yield stress in plastic disperse systems. Appl Phys Lett 82:3239–3241
34. Narine SS, Marangoni AG (1999) Mechanical and structural model of fractal networks of fat crystals at low deformations. Phys Rev E 60:6991–7000
35. Toro-Vazquez JF, Morales-Rueda JA, Dibildox-Alvarado E, Charó-Alonso MA, Alonzo-Macias M, González-Chávez MM (2007) Thermal and textural properties of organogels developed

by candelilla wax in safflower oil. J Am Oil Chem Soc 84:989–1000
36. Rogers MA, Wright AJ, Marangoni AG (2008) Crystalline stability of self–assembled fibrillar networks of 12-hydroxystearic acid in edible oils. Food Res Int 41:1026–1034
37. Campos R, Narine SS, Marangoni AG (2002) Effect of cooling rate on the structure and mechanical properties of milk fat and lard. Food Res Int 35:971–981
38. Dassanayake LSK, Kodali DR, Sato SU (2009) Physical properties of rice bran wax in bulk and organogels. J Am Oil Chem Soc 86:1163–1173
39. Morales-Rueda JA, Dibildox-Alvarado E, Charó-Alonso MA, Toro-Vazquez JF (2009) Rheological properties of candelilla wax and dotriacontane organogels measured with a true-gap system. J Am Oil Chem Soc 86:765–772